NASA/TM—2007-214956

Aerosol Measurements of the Fine and Ultrafine Particle Content of Lunar Regolith

Paul S. Greenberg
Glenn Research Center, Cleveland, Ohio

Da-Ren Chen
Washington University in St. Louis, St. Louis, Missouri

Sally A. Smith
Raytheon Missile Systems, Tucson, Arizona

September 2007

NASA STI Program . . . in Profile

Since its founding, NASA has been dedicated to the advancement of aeronautics and space science. The NASA Scientific and Technical Information (STI) program plays a key part in helping NASA maintain this important role.

The NASA STI Program operates under the auspices of the Agency Chief Information Officer. It collects, organizes, provides for archiving, and disseminates NASA's STI. The NASA STI program provides access to the NASA Aeronautics and Space Database and its public interface, the NASA Technical Reports Server, thus providing one of the largest collections of aeronautical and space science STI in the world. Results are published in both non-NASA channels and by NASA in the NASA STI Report Series, which includes the following report types:

- TECHNICAL PUBLICATION. Reports of completed research or a major significant phase of research that present the results of NASA programs and include extensive data or theoretical analysis. Includes compilations of significant scientific and technical data and information deemed to be of continuing reference value. NASA counterpart of peer-reviewed formal professional papers but has less stringent limitations on manuscript length and extent of graphic presentations.

- TECHNICAL MEMORANDUM. Scientific and technical findings that are preliminary or of specialized interest, e.g., quick release reports, working papers, and bibliographies that contain minimal annotation. Does not contain extensive analysis.

- CONTRACTOR REPORT. Scientific and technical findings by NASA-sponsored contractors and grantees.

- CONFERENCE PUBLICATION. Collected papers from scientific and technical conferences, symposia, seminars, or other meetings sponsored or cosponsored by NASA.

- SPECIAL PUBLICATION. Scientific, technical, or historical information from NASA programs, projects, and missions, often concerned with subjects having substantial public interest.

- TECHNICAL TRANSLATION. English-language translations of foreign scientific and technical material pertinent to NASA's mission.

Specialized services also include creating custom thesauri, building customized databases, organizing and publishing research results.

For more information about the NASA STI program, see the following:

- Access the NASA STI program home page at *http://www.sti.nasa.gov*

- E-mail your question via the Internet to *help@sti.nasa.gov*

- Fax your question to the NASA STI Help Desk at 301–621–0134

- Telephone the NASA STI Help Desk at 301–621–0390

- Write to:
  NASA Center for AeroSpace Information (CASI)
  7115 Standard Drive
  Hanover, MD 21076–1320

NASA/TM—2007-214956

Aerosol Measurements of the Fine and Ultrafine Particle Content of Lunar Regolith

Paul S. Greenberg
Glenn Research Center, Cleveland, Ohio

Da-Ren Chen
Washington University in St. Louis, St. Louis, Missouri

Sally A. Smith
Raytheon Missile Systems, Tucson, Arizona

National Aeronautics and
Space Administration

Glenn Research Center
Cleveland, Ohio 44135

September 2007

Acknowledgments

The authors would like to acknowledge the efforts of Fan Mei and Ta-Chih Hsiao at the University of Washington in St. Louis for their assistance in the calculation of experimental errors and in the preparation of figures.

This report contains preliminary findings, subject to revision as analysis proceeds.

Level of Review: This material has been technically reviewed by technical management.

Available from

NASA Center for Aerospace Information
7115 Standard Drive
Hanover, MD 21076–1320

National Technical Information Service
5285 Port Royal Road
Springfield, VA 22161

Available electronically at http://gltrs.grc.nasa.gov

Aerosol Measurements of the Fine and Ultrafine Particle Content of Lunar Regolith

Paul S. Greenberg
National Aeronautics and Space Administration
Glenn Research Center
Cleveland, Ohio 44135

Da-Ren Chen
Washington University in St. Louis
St. Louis, Missouri 63130

Sally A. Smith
Raytheon Missile Systems
Tucson, Arizona 85734

Abstract

We report the first quantitative measurements of the ultrafine (20 to 100 nm) and fine (100 nm to 20 μm) particulate components of Lunar surface regolith. The measurements were performed by gas-phase dispersal of the samples, and analysis using aerosol diagnostic techniques. This approach makes no *a priori* assumptions about the particle size distribution function as required by ensemble optical scattering methods, and is independent of refractive index and density. The method provides direct evaluation of effective transport diameters, in contrast to indirect scattering techniques or size information derived from two-dimensional projections of high magnification-images. The results demonstrate considerable populations in these size regimes. In light of the numerous difficulties attributed to dust exposure during the Apollo program, this outcome is of significant importance to the design of mitigation technologies for future Lunar exploration.

Nomenclature

C_c	Cunningham slip factor
D_d	Aerosol droplet diameter
D_p	Particle diameter
Kn	Knudsen number
n_e	Number of electrical charges carried by a particle
N	Particle number concentration
t_p	Particle transit time
U_g	Gas velocity
V_p	Particle velocity
Z_p	Particle electrical mobility
η	Dynamic viscosity
λ	Mean free path of gas molecules

1. Introduction

Prior to the initiation of the Apollo program, scientists and engineers were sensitive to the fine particulate nature of the surface regolith. Data from the preceding Surveyor [Choate, 1969] and Russian Luna missions [Heiken et al, 1991] afforded glimpses of unusual [by terrestrial standards] geotechnical properties. Numerous concerns over the tolerance of space flight systems to the particulate environment

emerged early on. One worst case scenario envisioned the Lunar Excursion Module (LEM) virtually disappearing below meters of the fine surface blanket [Cooper, 1969, 1970]. Indeed, as Apollo unfolded, a variety of particulate-related problems were observed. These included the degradation of space suit materials and bearings, compromised vacuum seals on sample return boxes, off-nominal performance of thermal emissive surfaces, and crew observations of ocular and respiratory irritation [Gaier, 2005]. The ubiquitous nature of the problem is captured in the remarks of Apollo 17 astronaut Gene Cernan, *"I think dust is probably one of our greatest inhibitors to a nominal operation on the Moon. I think we can overcome other physiological or physical or mechanical problems except dust"* [Apollo 17 Technical Debrief].

From this perspective, the comparatively short durations of the individual Apollo missions must now be viewed relative to NASA's New Vision for Space Exploration, and the goal of long term human presence on the Lunar surface [http://www.nasa.gov/pdf/55583main_vision_space_exploration.pdf]. A broad array of supporting systems suitably tolerant to the particulate environment must be developed and demonstrated. In general, limitations on payload mass launch capacity promote the need for components and assemblies capable of operation in the Lunar environment for extended periods, i.e., months or years. The number and complexity of surface systems will extend considerably beyond those developed for the Apollo Program, and by design must include infrastructure provisions for surface mobility, habitation, communication, fabrication and construction, geotechnical manipulation, and in-situ resource utilization. Further, the majority of these systems will experience thermal and radiative exposure cycles associated with the Lunar day/night cycle, and will likely operate at varying physical locations under unique conditions. Other factors and considerations arise, such as the increased demand placed on densely packed, static-sensitive microelectronics, the operational environment and performance requirements of thermal regulating systems, and possibly human health effects associated with long terms particulate exposure.

1.1 Rationale for this Study

While the aforementioned problems have been attributed to the presence of "Lunar Dust," a formal definition for this material remains lacking. A working definition can be taken as the size fraction smaller than 10 to 20 μm, below which the action of electrostatic and Van der Waals forces at surfaces dominate inertial effects [Bowling, 1986]. Similar sizes have been postulated for stable levitation of particulates within the Lunar plasma sheath [Colwell, 2001]. This same size range has more recently emerged in the context of human respiratory effects [Oberdorster, 2001]. The present nomenclature for sub-regimes stems from the field of respiratory toxicology, wherein ultrafine spans the range from 10 to 100 nm, and fine from 100 nm to 10 μm. Health issues associated with ultrafines continue to attract particular attention due to the observed ability to penetrate deep into the alveolar region and translocate into the interstitium [Oberdorster, 2001].

As the first interplanetary objects retrieved by Man, Lunar samples remain uniquely compelling. Their chemical, structural, physical and mechanical properties have been studied extensively [Cooper, 1969; Heiken et al., 1991]. However, characterization of the fine and ultrafine particle size distributions (PSDs) and related physical properties of materials in these size domains remains generally outstanding. The objective of developing suitably tolerant system and component technologies mandates an improved understanding of dust as a material, and its coupling to the local environment is essential for emulating test conditions in order to validate the viability of candidate technologies and mitigation strategies. As such, the fundamental measurements of dust properties reported here represents an important initial step in supporting efforts in the development of surface systems required for planned Lunar missions of extended duration.

1.2 Intrinsic Regolith Properties

Lunar surface regolith is described as a somewhat cohesive, fine-grained and loosely compacted clastic material, varying in color from light to dark grey. Its physical properties are primarily the result of mechanical disintegration of basaltic and anorthositic rock, caused by continuous meteoric impact and

bombardment by interstellar charged atomic particles. This situation contrasts fundamentally with terrestrial soil formation, mediated by the presence of oxygen, humidity, atmospheric wind, and a robust array of contributing biological processes. Characterizing the specific properties of these materials is essential to understanding the potential effects on human and mechanical systems, and the development of related countermeasures. The characterization of physical properties is also required for the development of suitable regolith simulants necessary to support testing and performance verification of Lunar surface systems and mitigation strategies.

Although quantitative size distributions remain uncertain, Lunar regolith, in principal, can be expected to contain fine and ultrafine particles in significant number densities. Prior results obtained by mechanical sieving demonstrate that on a mass basis, 95% is smaller than 1 mm, roughly 50% is smaller than 60 μm, and approximately 10 to 20% occurs below 20 μm. [Heiken et al., 1991]. For comparison, a PSD that assumes constant mass per unit size bin would underpredict the fractional number occurring in the size range below 20 μm by roughly a factor of 10^5.

Studies of the larger size fractions demonstrate that the complex process of regolith formation results in structural and compositional properties that are observed to correlate with age, location, and particle size [Heiken et al., 1991]. This behavior is generally attributed to space weathering, i.e., the environmental conditions surrounding airless bodies wherein the surface layer experiences implantation by solar wind, and the grain size is continually reduced via comminution, principally owing to micrometeoroid impaction. Systematic modal abundances of minerals and agglutinic glasses are also observed to correlate with particle size. Similar size dependence is observed in the I_s/FeO ratio, or maturity index, the proportion of iron occurring in the ground state as nanophase grains relative to the total amount of iron present in both ground and oxide states [Morris, 1978]. The relatively high abundance of nanophase iron leads to observed elevated magnetic susceptibilities for material below roughly 45 μm, relative to similar values for coarser fractions [Morris, 1976]. The ability to isolate and ultimately analyze particle properties as a function of size in the submicron regime is therefore of interest from a variety of perspectives, extending from fundamental aspects of planetary formation to the practicalities of Lunar exploration. The results of this study serve as an initiation point for more detailed compositional studies by characterizing the basic size spectrum of this material.

2. Measurement of the Particle Size Distribution (PSD) Function

The measurement of PSDs in the micrometer and nanometer regimes is familiar in the aerosol sciences, and a variety of approaches have been reported [Baron and Willeke, 2001]. The specific objectives and constraints of this study dictate the technical methodology most suited to this application. As stated, the task concerns quantifying the PSD of the combined fine and ultrafine size regimes. Simultaneously, the specified upper bound of 10 to 20 μm represents the smallest size addressed in prior analyses of both PSDs as well as structural and compositional properties. At the opposite end of the spectrum, no definitive information or predictive models are available to bound the smallest particle size that might be observed. In general, current techniques for particle size analysis afford a minimum resolvable diameter on the order of 2.5 to 10 nm. The desired goal is to display the resulting data as a continuous function throughout the entire range, while providing a single, consistent physical basis for the effective size parameter (e.g., transport diameter, as opposed to optical scattering efficiency, effective diffusion coefficient, projected area via image analysis, etc.). The selected measurement technique(s) and accompanying method of sample dispersion must therefore afford a dynamic range of four orders of magnitude, provide a consistent physical measure of size, and do so for a sample material for which no *a priori* information is known about the expected form of the inherent size distribution. In addition, the total sample size made available for these measurements was extremely limited, on the order of a few hundred milligrams.

Techniques based on optical scattering or absorption require *a priori* knowledge of the complex refractive index, and are sensitive to particle shape [van de Hulst, 1981]. Both quantities remain unknown for this material at these sizes. Ensemble scattering methods are additionally problematic for this

application due to dynamic range considerations (the dependence of optical scattering cross section on particle diameter), and the requirement to fit the resulting data to *ab initio* assumed functional forms for the PSD [Pecora, 1985]. Post analysis of two-dimensional projected SEM images is complicated by uncertainties in size-dependent sample collection efficiencies and contrast-dependent edge detection accuracies. For these reasons, the sequential measurement of aerodynamic transport diameters was selected, and determined directly using a Scanning Mobility Particle Sizer (SMPS; TSI Model 3080 Electrostatic Classifier with Model 3010S Detector) for the 2.5 to 500 nm range, and an Aerodynamic Particle Sizer (APS; TSI Model 3321) for the 500 nm to 20 μm range. Both techniques are mature and commonly used, and the underlying principles and embodiment widely referenced in the literature [Baron and Willeke, 2001].

2.1 Experimental Configuration

A functional diagram of the measurement apparatus used to perform the PSD measurements is shown in Figure 1. The SMPS determines aerodynamic transport diameter by virtue of measuring individual particle electrical mobilities, $Z_{p,}$:

$$Z_p = \frac{n_e \mathrm{C}_c(\mathrm{Kn})}{3\pi\eta D_p} \tag{1}$$

where n_e is the number of electrical charges carried by a particle of diameter D_p, $\mathrm{C}_c(\mathrm{Kn})$ is the Cunningham slip factor that accounts for noncontinuum effects when the particle size becomes comparable with or smaller than the mean free path of the surrounding gas, and η is the dynamic viscosity of the surrounding gas. The slip factor is a function of the Knudsen number , $\mathrm{Kn} = 2\lambda/D_p$, where λ is the mean free path of the gas molecules. The value of C_c is accurately determined using the empirical formulation of Allen and Raabe. [Baron and Willeke, 2001]. Equation (1) is independent of the particle density, negating the distinction between aerodynamic and Stokes diameters. Z_p expresses the ratio of electrical to viscous forces, and is the equilibrium velocity exhibited by a particle of diameter D_p in a gas of viscosity η under the presence of a unit electric field.

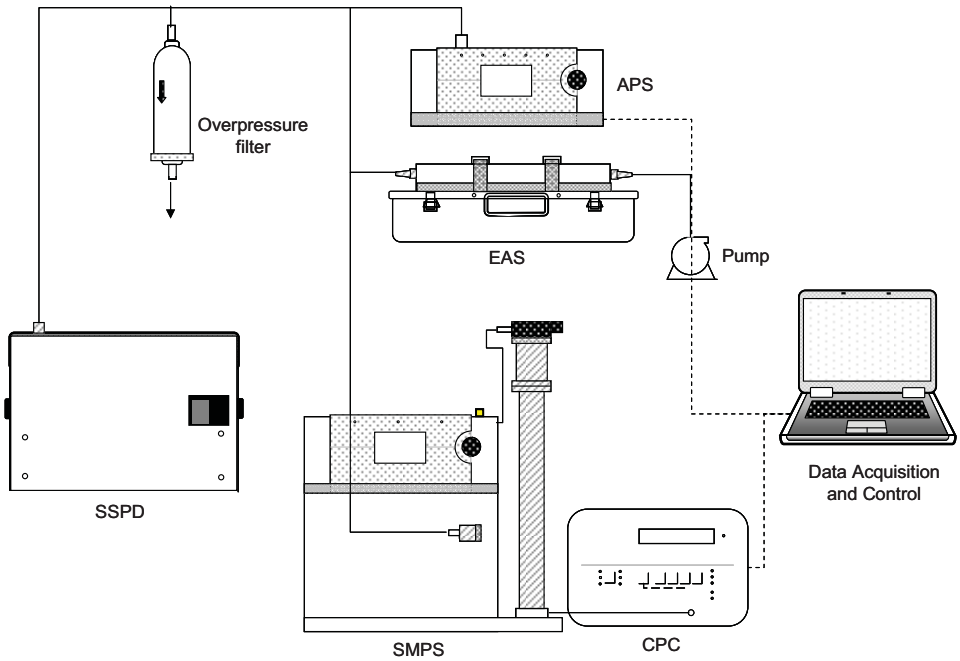

Figure 1.—Experimental configuration for PSD measurements.

It is seen from equation (1) that evaluating Z_p requires a knowledge of the particle electrical charge state. In the SMPS configuration utilized here, this electrical charge state distribution is achieved by subjecting the input sample stream to equilibrium bipolar diffusion charging. The exact form of the resulting distribution of charge states is well known, and has shown to be independent of particle composition. [Liu and Pui, 1974; Hussin et al., 1983; Liu et al., 1986; Wiedensohler et al, 1986; Adachiet al., 1993] The instrument used in this study employs the alpha emitter Kr85 as the source of ionizing radiation.

The SMPS consists of an electrostatic classifier, followed by a Condensate Particle Counter (CPC) for detection. The former utilizes the most common classifier configuration, a pair of coaxial cylinders across which an electrical potential is established [Hinds, 1999]. Particles to be analyzed are entrained in a laminar sheath gas oriented axially in the annular gap between the cylinders. The applied electric field exerts a radial force on the charged particles, deflecting their otherwise linear, stream-wise motion. The resultant trajectories depend uniquely on the individual particle mobilities. For a fixed geometry, flow rate, and applied potential, only particles of a specific mobility will exhibit the trajectory necessary to pass through the exit aperture and proceed to the CPC for detection. The mobility (and therefore size, from eq. (1)) distribution is obtained by sequentially varying the applied voltage while the axial gas stream velocity is held constant. In this fashion, the SMPS functions as a tunable, size-dependent, band-pass filter. The instrumental accuracy of the SMPS employed here is demonstrated to be 1% or better over the size range of interest [Mulholland et al., 2006].

Particles of the selected mobility value exit the classification column and are counted by the CPC. The CPC nucleates the incoming particles into individual supermicron droplets under a super-saturated vapor environment, effectively enhancing the threshold size that can be detected optically. [Baron and Willeke, 2001]. By establishing the proper saturation ratio, the particles serve as nucleation centers for condensate droplet growth, and as such the CPC is capable of single particle detection and provides a one-to-one mapping between the number of incoming particles and the number of droplets formed. A computer is used to sequentially scan the voltage applied to the classification column, and simultaneously record the number of particles of corresponding mobility counted by the CPC.

The APS determines the aerodynamic transport diameter by measuring the time-of-flight (TOF) of particles entrained in an accelerating gas flow [Chen , 1985]. The resulting lag between the gas and particle velocities, respectively, is a function of the particle diameter. TOF of individual particles is measured by a pair of laser beams axially focused on the exit region of the acceleration nozzle. Light scattered by the particles is collected by an avalanche photodiode, and the observed spacing between the two optical pulses is used to accurately measure the transit time through the optical sample volume. The observed velocity lag is independent of particle density within the Stokes regime, and non-Stokesian corrections have been developed [Wang and John, 1987; Ananth and Wilson, 1988]. An assumed worst case value of 2.85 g/cm^3 [Heiken et al, 1991] provides a density correction of less than 8% for particles of 15 μm diameter, and for diameters of 5 μm and smaller this correction is small compared to the inherent instrumental accuracy. On a number density basis, the samples as provided displayed relatively little content for diameters greater than 5 μm , rendering the effect of density corrections negligible.

Each APS instrument is calibrated with precision reference spheres at the point of manufacture to account for slight variations in the dimensions and spacings of internal components, such as the accelerating nozzle and laser beam spacing. The Bernoulli equation for compressible flow is used to calculate U_g, the gas velocity, as a function of the pressure differential across the nozzle, where the latter is used as an internal control monitor to insure that U_g is maintained at a constant value. In the Stokes regime, $t_p \sim V_p/U_g$, where t_p is the particle transit time through the sample volume, and V_p is the particle velocity. Plotting the ratio of V_p/U_g as a function of the Stokes number results in a universal response curve, such that the APS size response under varying conditions of pressure or viscosity is preserved by maintaining U_g at the set-point value [Chen et al., 2004].

The most common source of error in an APS is attributable to coincidence effects. [Baron and Willeke, 2001]. Such errors are more prevalent at high concentrations, and occur when more than one particle is present in the sample volume during the nominal timing interval. The APS instrument utilized

here contains a number of provisions for the detection and elimination of coincidence artifacts, including the simultaneous measurement of scattered optical power for correlated validation of each individual size detection event. While coincidence errors are logged and can be used as a basis to correct the measured distributions, the particle concentrations in this study were relatively low, resulting in the extremely infrequent occurrence of detected coincidence events. The instrumental accuracy of the APS employed here is demonstrated to be 2% or better over the size range of interest [Chen et al., 1984; 1985]

2.2 Sample Dispersion

The measurement of aerosol PSDs requires a method for sample dispersal and delivery to the analysis instruments. In principal, the process of dispersal, should effectively deagglomerate but not fracture the material, while minimizing particle losses and the introduction of size-dependent biases. This application involves the additional challenges of dispersing a sample containing particles which potentially span four orders of magnitude in diameter and of severely limited quantity, and the desire to simultaneously deliver the batch sample to three analysis instruments in parallel. Aerosol dispersion from liquid-phase is at once problematic, due to the difficulty in minimizing the occurrence of agglomerate states. The statistical occurrence of agglomerates as a function of D_p/D_d, particle diameter to dispersed droplet diameter, can be predicted and optimized, the latter aided by a variety of techniques for producing droplets of specified and controlled sizes. Doing so for the particle size range of interest here, however, renders this an impossibility in practice. [Baron and Willeke, 2001]. Liquid suspensions also present the possibility of artifacts from residual contaminants, complicated in this case by the inability to post filter the data based on the expected particle PSD. These aspects aside, attempts in the laboratory at producing stable liquid-phase particle suspensions proved unsatisfactory, as the rapid sedimentation of larger sizes was visually apparent, despite provisions for active stirring and ultrasonic mixing.

For these reasons, direct dispersion and aerosolization from the dry powder phase was implemented using a coaxially entrained Small Sample Particle Disperser (SSPD; TSI Model 3433) [Blackford and Rubow, 1986]. The design of the mixing throat in this device deagglomerates the dry sample via aerodynamic shear stresses, while minimizing internal losses. To validate effective sample deagglomeration, the aerosol stream was simultaneously directed to an Electrical Aerosol Sampler (EAS; TSI Model 3100). The EAS deposits the sample material onto electron microscopy grids for subsequent image analysis, and utilizes both static and dynamic electrophoretic effects to increase collection efficiency and minimize spatial biases across the active area of the grids. [Fissan et al., 1983]. The volumetric flow rate of the SSPD was set to approximately 20 lpm to insure effective dispersal in the mixing throat. The HEPA (high efficiency particle air filter) overpressure filter internal to the SSPD was capped, and a separate overpressure filter was placed downstream close to the input of the analysis instruments to minimize losses by maximizing entrainment. The 20 lpm generated by the SSPD overfills the combined capacity of the SMPS, APS, and EAS, such that the HEPA filter bleeds off the excess capacity while allowing each instrument to operate at its specified volumetric input capacity.

3. System Calibration and Regolith Sample Measurements

Before proceeding with the regolith material, measurements were performed on a number of reference samples to validate the instrumental calibration constants and end-to-end performance of the complete system. For both the SMPS and APS, a series of monodisperse polystyrene latex spheres (PSL; Duke Scientific Series 3000 and 4000 Certified Particle Size Standards) of varying diameters throughout their respective ranges were aerosolized from liquid-phase suspension using a collision atomizer. In all cases, the measured diameters were within the stated accuracy of the respective instruments. The APS was further tested by dispersing a dry powder sample of SAE Medium Dust using the SSPD. Although no formal polydisperse powder reference standard is available, the results were in close agreement with the manufacturer's measured PSD, despite the latter being obtained with a differing measurement technique, i.e., in liquid phase suspension using a Coulter counter. No comparable polydisperse sample is available

in the ultrafine domain. Combined APS and SMPS data characterizing end-to-end system performance using aerosolized NaCl solutions is described later in this section.

Plotting the composite data in absolute units necessitates a method for matching the two parallel data sets at the size transition boundary. The operation of combining the data sets was performed in software using the DataMerge® (TSI product #390069) [Han et al., 2005], an application tailored to merging data simultaneously collected by the SMPS and APS instruments. The first operation corrects the APS data to compensate for the differences in volumetric throughput and effective measurement bin widths. The data from both instruments can be fit to a variety of multi-parameter distributions prior to merging, and the combined data set can be fit to a multi-modal distribution model as well. However, these features were not utilized here, since no explicit form for the PSD could be assumed *a priori*. The corrected APS data is then scaled to match the SMPS data by comparing the sum of the total number counts for all particle detection events in the size overlap region for the two instruments. This overlap region extended from 523 to 644 nm, the former value being set by the lower size cutoff of the APS, and the latter value corresponding to the upper size limit of the SMPS. In principal, the particular SMPS classification column used for this study is nominally capable of measuring larger particles. The value of upper size limit is determined by the combination of sheath and sample volumetric flows, and maximum applied voltage, and was chosen to optimize the instrumental resolution while simultaneously minimizing particle losses at the small end of the size spectrum. Measured PSDs were corrected for size-dependent losses internal to the instruments [Peters and Volckens, 2005; Reineking and Porstendörfer, 1986]. Corrections for size-dependent diffusion losses in all delivery tubing were determined experimentally by direct measurement, using a scanned 3080 classifier for sequential monodisperse particle generation, and two 3010S CPCs for detection.

The data merging algorithms were validated using a test aerosol of NaCl particles dispersed from liquid solution. First, a diluted 0.25% (by volume) NaCl solution was aerosolized in a collision atomizer to generate a PSD lying completely within the range of the SMPS. A second 18% NaCl solution was then aerosolized with the same atomizer operating under identical conditions. The additional dilution value was chosen to provide a PSD with a peak value of 389 nm, occurring near the transition boundary of the SMPS and APS. As observed in Figure 2, the combined PSD rolls off smoothly towards both extrema as expected, and the merging process does not bias the measured sample standard deviation.

Two samples of Lunar surface regolith were then analyzed with this combined system, with care being taken to preserve the exact configuration used for the calibration procedures (e.g., the exact geometry, length, and materials of all delivery tubing and associated couplings). The first, designated 10084, was manually collected by Neil Armstrong during Apollo 11. Sample 70051 was deposited on the surface of the Lunar rover, and subsequently collected by Harrison Schmitt on Apollo 17. The Apollo 11 Mission landed well within a mare basalt region, whereas the landing sight of Apollo 17 corresponds to the juncture of the mare plains and highland hills. However, considerable variations in regolith properties are often observed within a single site, and mature (old) and immature (young) samples are found to occur within the same area, exhibiting differing mineralogical properties [Simmons et al., 1972; Papike et al., 1981; Englehardt et al., 1976; McKay et al., 1976]. Details concerning the origin, acquisition, handling, post-processing, and storage of these materials can be obtained from the office of the NASA Lunar Sample Curator [http://curator.jsc.nasa.gov/index.cfm]. In this study, both samples were mechanically sieved at the 20 μm level prior to receipt.

4. Results and Discussion

The measured PSDs of the Lunar regolith samples are shown in Figure 3, where the *x*-axis is the natural logarithm of the particle diameter (D_p), and the *y*-axis is the number of particles/cm^3 occurring in a bin of width $\log(D_p)$. In the upper panels, the measured data is plotted without error bars for clarity. The most notable observation is the occurrence of significant submicron populations in both samples, representing the first reported quantitative measurements of ultrafine content in Lunar regolith. Also

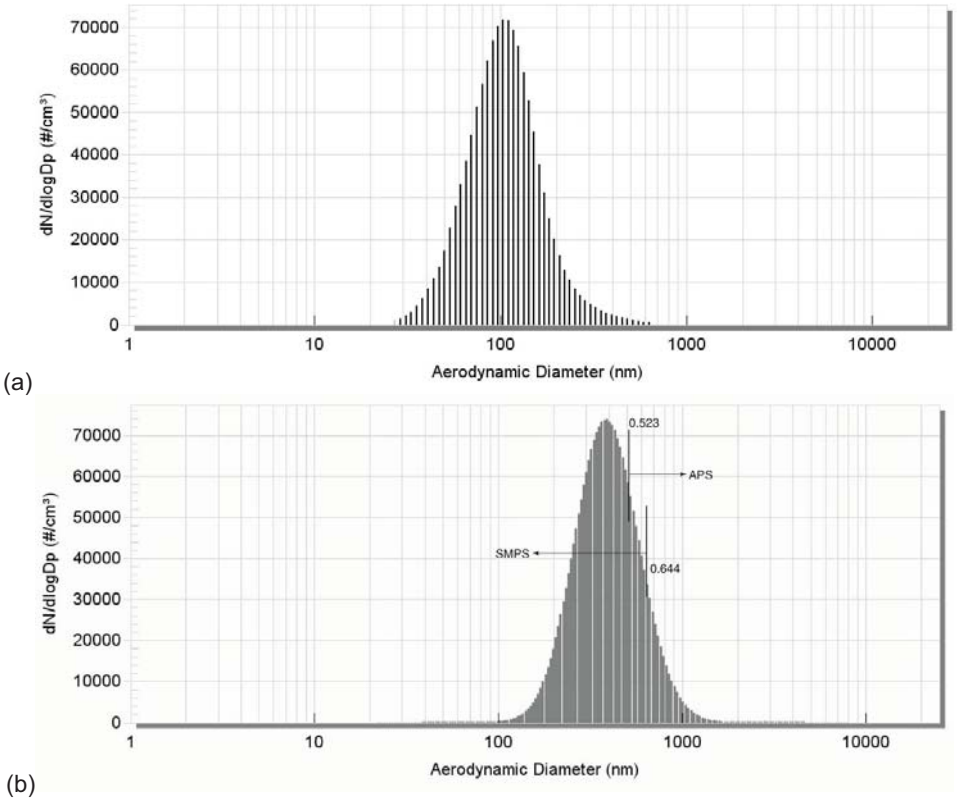

Figure 2.—(a) SMPS data: mode maximum diameter of 102 nm, σg = 1.58; 0.25% NaCl solution. (b) Composite plot of merged data from SMPS and APS instruments: mode maximum diameter of 392 nm, σg = 1.59; 18% NaCl solution.

observed are bimodal distributions displaying principal peaks occurring at approximately 1.1 to 1.2 μm and 300 to 400 nm, respectively. The maximum values for both peaks occur at slightly larger values in sample 70051, which also exhibits a relatively higher abundance of the ultrafine fraction. The distribution of fines in 70051 is also observed to decay more rapidly with increasing particle diameter. As received, both samples contained relatively few particles either smaller than 40 nm or larger than 5 μm.

The error bars correspond to the relative standard deviation, and are calculated directly from the measured data for each size bin. The data represents the average of four independent sets, where each set consisted of five sequential scans of the SMPS. The scan rate of the SMPS is chosen to balance the instrumental resolution and bin counting statistics, and this, in combination with the total amount of available sample material, determines the total number of allowable scans. The comparative magnitude of the observed standard deviations reflect the different counting statistics for the two instruments. As the SMPS is sequentially scanned across its respective size range, only particle events falling within its instantaneous passband are recorded. In contrast, the APS sizes and records all particle arrivals as they occur.

It should be noted that measured PSDs reflect the integrated history of the sample. The present scientific interest in fine particulates largely post-dates the Apollo program, and specific provisions for handling and post-processing to minimize losses and size-dependent sample biases were essentially absent at that time. PSDs are readily altered by handling and post-processing, including the introduction of bimodalities [Zimmer and Maynard, 2002]. The structure and similarities in these data sets may in part be traceable to similarities in the treatment of the two samples after the fact. In general, the smallest size fractions are preferentially lost upon handling and post-processing, promoting the values observed here as conservative estimates. This is particularly the case for the ultrafine regime. The noted absence of number densities in both samples occurring below 40 nm must be viewed with some care in this regard.

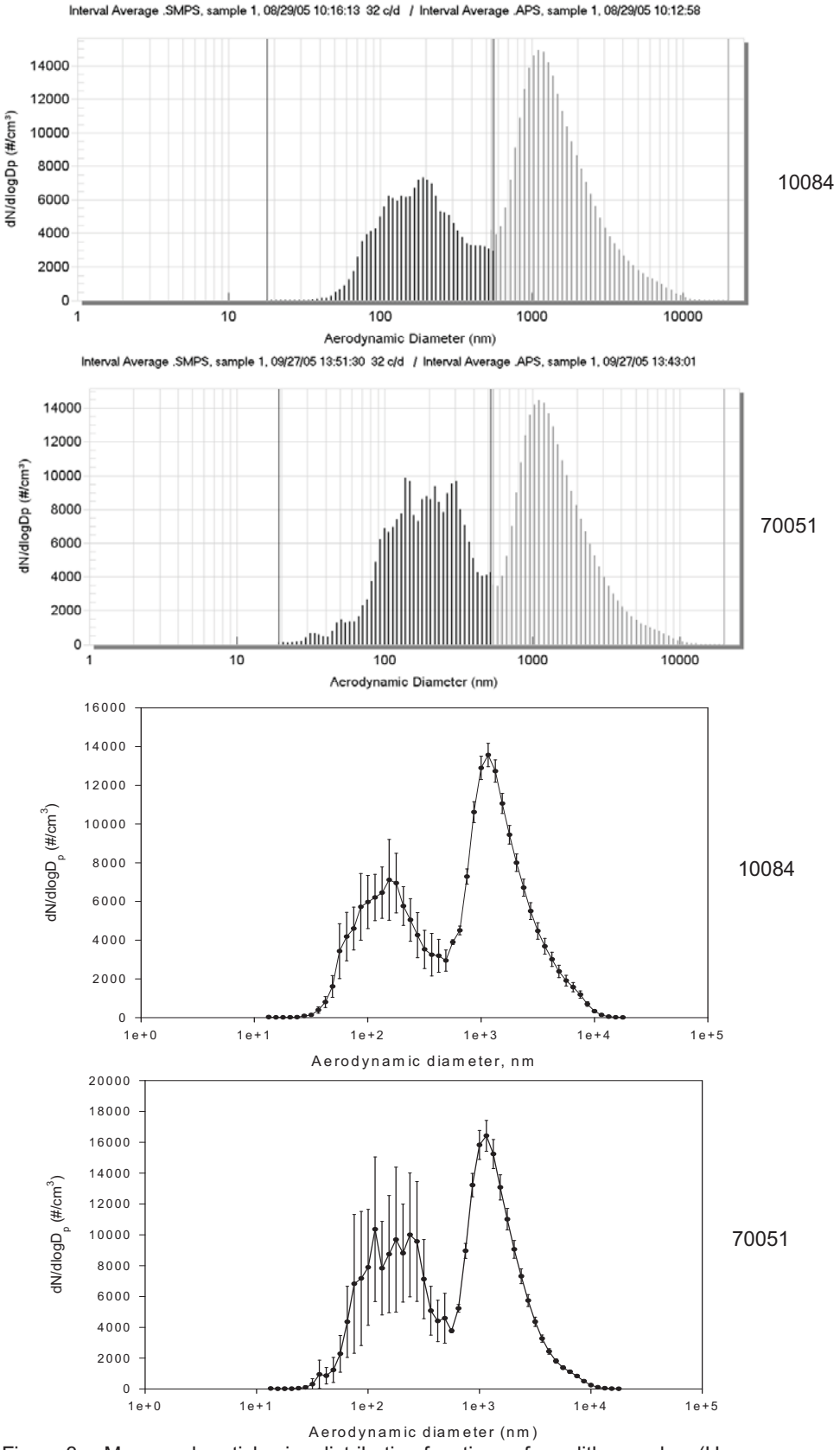

Figure 3.—Measured particle size distribution functions of regolith samples. (Upper panels shown without error bars for clarity.)

It should be noted that measured PSDs reflect the integrated history of the sample. The present scientific interest in fine particulates largely post-dates the Apollo program, and specific provisions for handling and post-processing to minimize losses and size-dependent sample biases were essentially absent at that time. PSDs are readily altered by handling and post-processing, including the introduction of bimodalities [Zimmer and Maynard, 2002]. The structure and similarities in these data sets may in part be traceable to similarities in the treatment of the two samples after the fact. In general, the smallest size fractions are preferentially lost upon handling and post-processing, promoting the values observed here as conservative estimates. This is particularly the case for the ultrafine regime. The noted absence of number densities in both samples occurring below 40 nm must be viewed with some care in this regard.

As discussed, the grids collected by the EAS were subject to SEM analysis to validate the effectiveness of the SSPD in de-agglomerating the bulk sample. A random sampling of several hundred particle images revealed only two occurrences of agglomerate structures. No indication of mechanical fracturing or degradation of individual particles from the dispersal process was observed. An image of one agglomerate structure is shown in figure 4. While it is undetermined whether this structure was fused together by naturally occurring Lunar surface processes, or as a result of insufficient shear forces within the SSPD, the observed infrequency of these chains tends to rule out the probability of the latter.

The SEM images are also of interest insofar as evaluating the relationship of the measured transport diameters to the true particle dimensions, since shape factors can significantly influence aerodynamic properties. Figures 5 and 6 depict typical particle shapes observed to occur in approximately 2.5 μm and 100 nm size ranges respectively. To first order, the images do not reveal complex or rod-like features that would result in significant departures between the aerodynamic and physical dimensions.

Various terrestrial processes result in the production of submicron particles, but are of a fundamentally different nature than the bombardment and agglutination mechanisms in the Lunar environment. These include ejecta from volcanic plumes [Rose et al., 1982], abrasive comminution in sandstorms [Park and Lee, 2004], and combustion products from large-scale forest fires [Brock, 2004]. Many of the same issues associated with fine and ultrafine particulates also apply to Lunar exploration, including the vulnerability of mechanical systems, obscuration of optical surfaces, electrical charge transfer, and respiratory health effects. Correlations between size and structural and compositional features are observed in the supermicron components of Lunar regolith, promoting interest in extending such analyses to the submicron fraction identified in this study. Thus, the observations reported here will support more detailed analysis of global regolith properties, with potential implications for both the scientific and engineering communities.

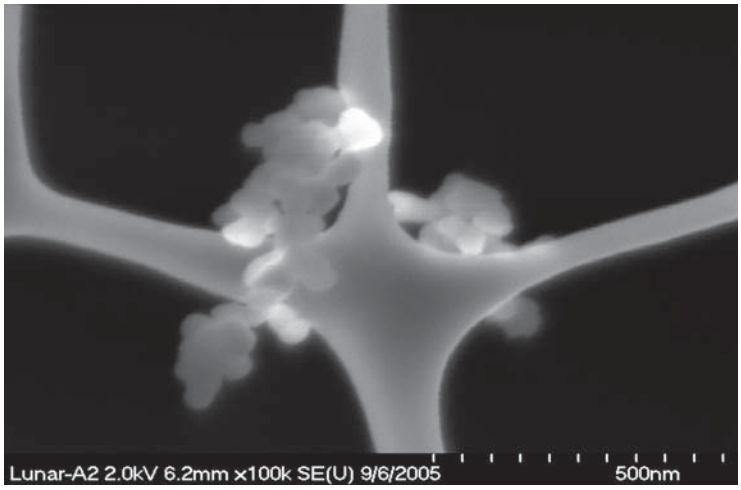

Figure 4.—Observed agglomerate structure via SEM.

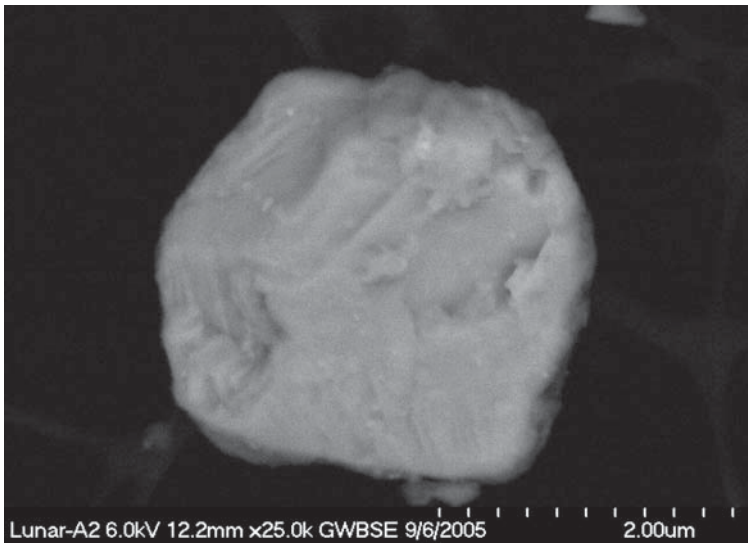

Figure 5.—Typical particle shape in supermicron regime.

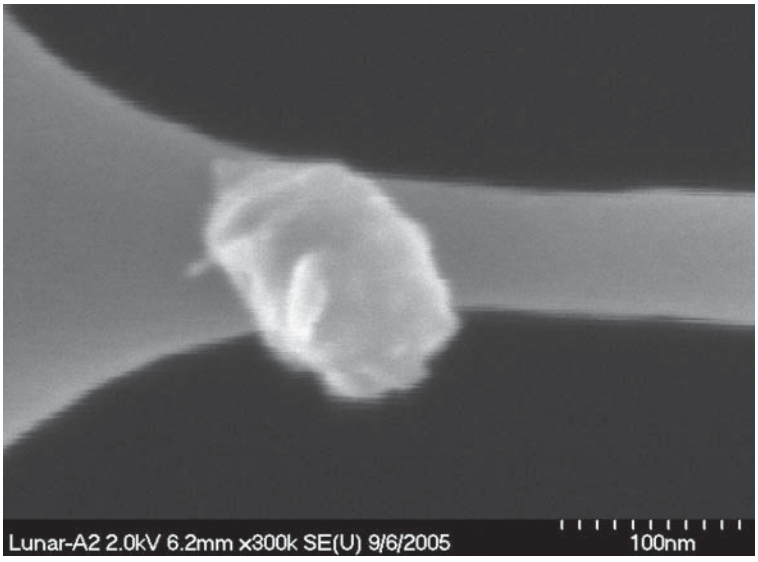

Figure 6.—Typical particle shape in submicron regime.

5. Summary

The perceived problem of Lunar dust is receiving renewed interest in anticipation of planned Lunar missions. Present mission profiles include provisions for extended human presence, promoting a need to assess and mitigate the potentially deleterious affects of dust on both surface systems and personnel. The results here represent the first reported quantitative measurements of the particle size distributions (PSDs) of Lunar surface regolith in the ultrafine and fine size regimes. This data is necessary for the design and testing of suitably tolerant components and systems supporting a variety of surface operations and amenities for human habitation. The measurement of PSDs provides important insight into the innate material, as well as constituting a useful step in the characterization of related size-dependant properties.

A number of techniques have been demonstrated for the measurement of particle size in this domain, and the techniques selected for this study were chosen to balance a variety of factors. These factors include a lack of precise specification of intrinsic particle properties (e.g., density and refractive index),

the absence of an *a priori* function form for the anticipated PSD, the potentially wide dynamic range in size, and the relatively small amount of sample available.

Two samples of Lunar surface regolith were characterized; sample 10084 [Apollo 11], and sample 70051 [Apollo 17]. Both demonstrate considerable populations on a number density basis throughout the ultrafine and fine regimes, with relatively small populations occurring in the ranges smaller than 40 nm or larger than 5 μm. It is noted that the samples were mechanically sieved at the 20 μm level prior to receipt, and that the inclusive history of the samples' acquisition, storage, handling, and processing remains somewhat incomplete insofar as the respective influence on the measured PSDs. In general, the propensity for increased particle losses with decreasing size due to both diffusion mechanisms and relative adhesion strengths promotes these measurements as conservative estimates of particulate content in the ultrafine and fine ranges.

The aerosolized samples were simultaneously collected on grids for SEM analysis to assess effective sample agglomeration and shape factors influencing the measured values of aerodynamic transport diameter. Since only two agglomerate structures could be identified, it is hypothesized that these structures were fused by *in situ* Lunar surface properties. None of the particle images examined were seen to exhibit shape factors sufficient to cause significant departures between the physical and measured diameters.

References

Adachi, M., D.Y.H. Pui, and B.Y.H. Liu (1993), Aerosol charge neutralization by a corona ionizer, *Aerosol Sci. and Tech*., 18, pp. 48–58.

Baron, P.A. and K. Willeke (2001), *Aerosol Measurements,* John Wiley & Sons, New York, 2nd ed., pp. 508–519 and 537–564.

Blackford, D.B., and K.L. Rubow (1986), *TIZ-Fachberiche*, 110 (10), pp. 645–655.

Bowling, R.A., in *Particles on Surfaces 1*, K.L. Mittal, (Ed.) (1986), Plenum Press, New York, pp. 129–142.

Brock, C.A., A.G. Wollny, O.R. Cooper, F.C. Fehsenfeld, J.A. de Gouw, P.K. Hudson, B.M. Matthew, A.M. Middlebrook, D.M. Murphy, R. Peltier, C. Simons, A. Stohl, A. Sullivan, C. Warneke, R.J. Weber, and J.C. Wilson (2004), Chemical and microphysical properties of particles in aged forest fire plumes from Alaska and Western Canada observed over the Northeastern U. S., paper presented at the American Geophysical Union Fall Meeting, Abstract #A31C–0070.

Chen, B.T., Y.S. Cheng, and H.C. Yeh, Performance of a TSI aerodynamic particle sizer (1985), *Aerosol Sci. and Tech*., 4, pp. 89–97.

Chen, D-R, S. C. Chen, C.-H. Huang, and C.-J. Tsai (2004) Universal calibration curve for the TSI aerodynamic particle sizer, *Aerosol Sci. and Tech*., 5, pp. 467–474.

Choate, R., S.A. Batterson, E.M. Christensen, R.E. Hutton, L.D. Jaffe, R.H. Jones, H.Y. Ko, R.F. Scott, R.L. Spencer, F.B. Sperling, and G.H. Sutton, Lunar Surface Mechanical Properties, in *Surveyor Program Results*, NASA SP–184, p. 129 (1969).

Colwell, J.E., S. Batiste, M. Horányi, S. Robertson, and S. Sture, (2006), The Lunar Surface: Dust Dynamics and Regolith Mechanics, accepted for publication in *Reviews of Geophysics* (submitted Sep. 16, 2006).

Cooper, H.S.F. Jr. (1969) *Apollo on the Moon,* Dial, New York, p. 144.

Cooper, H.S.F. Jr. (1970) *Moon Rocks,* Dial, New York, p. 197.

Engelhardt, W., H. Hurrle, and E. Luft (1976), Microimpactinduced changes of textural parameters and modal composition of the lunar regolith. *Proc. Lunar Sci. Conf. 7th,* pp. 373–392.

Fissan, H.J., C. Helsper, and H.J. Thielen (1983), Determination of Particle Size Distribution by Means of an Nanometer Aerosol Sampler, *J. of Aerosol Sci.*, 14, p. 354.

Gaier, J.R. (2005), The Effects of Lunar Dust on EVA Systems During the Apollo Missions, NASA/TM—2005-213610/REV1.

Gormley, P.G. and M. Kennedy (1949), Diffusion from a stream flowing through a cylindrical tube, *Proceedings of the Royal Irish Academy*, 52A, pp. 163–169.
Han, H.S., E.R. Whitby, D.B. Plate, and D.P. Albertson (2005), Combining TSI Scanning Mobility Particle Sizer and Aerodynamic Particle Sizer for Wide Range Particle Size Distribution Measurement, *European Aerosol Conference Poster Presentation*, Ghent, Belgium.
Heiken, G.H., D.T. Vaniman, and B. M. French (1991), *Lunar Sourcebook ,*Lunar Planetary Institute, Houston, TX, pp. 285–356.
Hinds, W.C. (1999), *Aerosol Technology*, John Wiley & Sons, New York, pp. 341–345.
http://curator.jsc.nasa.gov/index.cfm.
http://www.nasa.gov/pdf/55583main_vision_space_exploration.pdf
van de Hulst, H.C., (1981), *Light Scattering by Small Particles*, Dover, New York, 2nd ed., pp. 63–81.
Hussin, A., H.G. Scheibel, K.H. Becker, and J. Porstendorfer (1983), Bipolar diffusion charging of aerosol particles – I: Experimental results within the diameter range 4 – 30 nm, *J. Aerosol Sci*., 14, pp. 671–677.
Liu, B.Y.H., K.T. Whitby, and H.S. Yu (1967), *Review of Sci. Instruments*, 38 (1), pp. 100–102.
Liu, B.Y.H., and D.Y.H. Pui, Electrical neutralization of aerosols, *J. of Aerosol Sci.*, 5, pp. 465–472.
Liu, B.Y.H., and D.Y.H. Pui (1986), Aerosol charge neutralization by a radioactive alpha source, *Part. Charact*. 3, pp. 111–116.
McKay, D.S., G.H. Heiken, R.M. Taylor, U.S. Clanton, D.A. Morrison, and G.H. Ladle (1972), Apollo 14 soils: Size distribution and particle types, *Proc. Lunar Sci. Conf. 3rd,* pp. 983–995.
Morris, R.V. (1976), Surface exposure indices of lunar soils: A comparative FMR study, *Proc. Lunar and Planet Sci. Conf. 7th*, pp. 315–335.
Morris, R.V. (1978), Surface exposure (mature) of lunar soils: Some concepts and Is/FeO compilation, *Proc. Lunar Planet Conf. 9th*, pp. 2287–2297.
Mulholland, G.W., M.K. Donnelly, C.R. Hagwood, S.R. Kukuck, and V.A. Hackley (2006), Measurement of 100 nm and 60 nm Particle Standards by Differential Mobility Analysis, *J. Res. Natl. Inst. Stand. Technol*., 111, pp. 257–312.
Papike J.J., S.B. Simon, C. White., and J.C. Laul, (1981), The relationship of the lunar regolith <10 mm fraction and agglutinates. Part I: A model for agglutinate formation and some indirect supportive evidence, *Proc. Lunar Planet. Sci.* 12B*,* pp. 409–420.
Park, S., and E. Lee. (2004), Parameterization of Asian dust (Hwangsa) particle-size distributions for use in dust emission models, *Atmospheric Environment*, 38, pp. 2155–2162.
Pecora, R.P. (1985), *Dynamic Light Scattering, Plenum Press*, New York, pp. 46–47.
Peters, T.M., and J. Volckens, (2005), Counting and particle transmission efficiency of the aerodynamic particle sizer, *J. of Aerosol Sci.,* 36, 12, pp. 1400–1408.
Reineking, A. and Porstendörfer, J. (1986). Measurements of Particle Loss Functions in a Differential Mobility Analyzer (TSI, Model 3071) for Different Flow Rates. *Aerosol Science and Technology,* 5**,** pp. 483–486.
Rose, W.I., R.L. Chuan, and D.C. Woods (1982), Small particles in the plume of Mount St. Helens, *J. of Geophysical Research*, 87, pp. 4956–4962.
Simmons G., D.W. Strangway, L. Bannister, R. Baker, D. Cubley, G. La Torraca G., and R. Watts (1972), The surface electrical properties experiment, in *Lunar Geophysics,* Z. Kopal and D.W. Strangway, (Eds.), Reidel, Dordrecht, pp. 258–271.
Wiedensohler, A., E. Luktmeier, M. Feldpausch, and C. Helsper (1986), Investigation of the bipolar charge distribution at various gas conditions, *J. Aerosol Sci*., 17 (3), pp. 413–416.

REPORT DOCUMENTATION PAGE	Form Approved OMB No. 0704-0188

1. REPORT DATE *(DD-MM-YYYY)*	2. REPORT TYPE	3. DATES COVERED *(From - To)*
01-09-2007	Technical Memorandum	

4. TITLE AND SUBTITLE
Aerosol Measurements of the Fine and Ultrafine Particle Content of Lunar Regolith

5a. CONTRACT NUMBER

5b. GRANT NUMBER

5c. PROGRAM ELEMENT NUMBER

6. AUTHOR(S)
Greenberg, Paul, S.; Chen, Da-Ren; Smith, Sally, A.

5d. PROJECT NUMBER

5e. TASK NUMBER

5f. WORK UNIT NUMBER
WBS 321878.04.07.03.06

7. PERFORMING ORGANIZATION NAME(S) AND ADDRESS(ES)
National Aeronautics and Space Administration
John H. Glenn Research Center at Lewis Field
Cleveland, Ohio 44135-3191

8. PERFORMING ORGANIZATION REPORT NUMBER
E-16109-1

9. SPONSORING/MONITORING AGENCY NAME(S) AND ADDRESS(ES)
National Aeronautics and Space Administration
Washington, DC 20546-0001

10. SPONSORING/MONITORS ACRONYM(S)
NASA

11. SPONSORING/MONITORING REPORT NUMBER
NASA/TM-2007-214956

12. DISTRIBUTION/AVAILABILITY STATEMENT
Unclassified-Unlimited
Subject Categories: 91, 88, and 35
Available electronically at http://gltrs.grc.nasa.gov
This publication is available from the NASA Center for AeroSpace Information, 301-621-0390

13. SUPPLEMENTARY NOTES
Submitted to the Journal of Geophysical Research.

14. ABSTRACT
We report the first quantitative measurements of the ultrafine (20 to 100 nm) and fine (100 nm to 20 μm) particulate components of Lunar surface regolith. The measurements were performed by gas-phase dispersal of the samples, and analysis using aerosol diagnostic techniques. This approach makes no a priori assumptions about the particle size distribution function as required by ensemble optical scattering methods, and is independent of refractive index and density. The method provides direct evaluation of effective transport diameters, in contrast to indirect scattering techniques or size information derived from two-dimensional projections of high magnification-images. The results demonstrate considerable populations in these size regimes. In light of the numerous difficulties attributed to dust exposure during the Apollo program, this outcome is of significant importance to the design of mitigation technologies for future Lunar exploration.

15. SUBJECT TERMS
Lunar regolith; Particle size measurements; Particle measurement technology; Ultrafine particles

16. SECURITY CLASSIFICATION OF:			17. LIMITATION OF ABSTRACT	18. NUMBER OF PAGES	19a. NAME OF RESPONSIBLE PERSON
a. REPORT	b. ABSTRACT	c. THIS PAGE			STI Help Desk (email:help@sti.nasa.gov)
U	U	U	UU	19	19b. TELEPHONE NUMBER *(include area code)* 301-621-0390